

Evaluation of Corrosion Resistance Properties of Hexagonal Boron Nitride Based Polymer Composite Coatings for Carbon Steel in a Saline Environment

Fadhel T. Alabdullah^{1,†}, C. Ali², and Brajendra Mishra³

¹Department of Mechanical Engineering, College of Engineering, AlAsala Colleges, Saudi Arabia

²Department of Metallurgical and Materials Engineering, Colorado School of Mines, CO, USA

³Mechanical Engineering, Worcester Polytechnic Institute, MA, USA

(Received May 27, 2021; Revised November 23, 2021; Accepted November 24, 2021)

Herein, we report polyvinyl butyral composites coatings containing various loadings of 72-h bath sonicated hexagonal boron nitride particles (5 μm) to enhance barrier properties of coatings. Barrier properties of coatings were determined in 3.5 wt% NaCl after different time periods of immersion via electrochemical techniques such as open circuit potential, electrochemical impedance spectroscopy, and potentiodynamic polarization test. Coatings containing sonicated hexagonal boron particles exhibited improved corrosion resistance for longer periods of immersion compared to neat coating. We also discussed effects of hexagonal boron nitride on healing properties of polyvinyl butyral. Coatings containing 1.0 wt% loading of sonicated hexagonal boron nitride showed improved long-term barrier properties than coatings with other compositions. The presence of hexagonal boron nitride also affected the healing properties of polyvinyl butyral coatings besides their barrier properties. Such improved barrier properties of composites coatings were attributed to the high aspect ratio, plate-like shape, and electrically insulated nature of the filler.

Keywords: Coating, h-BN, EIS, OCP, Carbon steel, Polymer

1. Introduction

Generally, carbon steel containing various percentage of carbon is considered economical and used as major alloy for many applications such long pipelines and vessels. Severe environments make carbon steel more vulnerable towards corrosion, hence, limiting its practical applications [1]. Coating a metallic surface is one of the widely used techniques used for decorative surface finish and corrosion protection [2]. To enhance the physicochemical properties and corrosion protection ability of the polymer coatings, different fillers/pigments are incorporated into the coatings formulations [3]. Depending on the final applications of metals and protection mechanism, corrosion inhibitors/fillers, can be classified as organic and inorganic [4]. The main protection mechanism offered by barrier fillers/plate-like fillers is to provide tortuous paths for the electrolyte, which delay the corrosion process [5-7]. The presence of plate-like fillers can provide the longest way for the corrosive solution to reach at the coating substrate interface which may delay the corrosion process [8-13].

Hexagonal form of boron nitride (h-BN) analogous to graphite is a three-dimensional (3-D) layered material comprising of thin sheets stacked together through weak van der Waals force. Similarly, to graphite, h-BN is also used in many applications such as solid lubricants, ultraviolet light emitter etc. Also, the h-BN structure with exposed 002 crystal plane would have similar properties as graphitic-like (002) plane including excellent thermal conductivity and mechanical strength. The polymer resin commercially names Butvar-98 used in this study is mostly composed of polyvinyl butyral copolymer with vinyl acetate and vinyl alcohol. The hydrophilic nature and reactive hydroxyl sites facilitate adhesion and crosslinking ability for coatings application. Also, the PVB resin is soluble in wide range of solvents such as methanol, ethanol, isopropyl alcohol and many other polar solvents. Further, the improvement of properties in coated Butvar resin can be done using cross-linking reaction through transacetalization and other complex mechanisms during curing [14].

Much research work has been reported on the inclusion of sheet/plate like structure fillers such as graphene to

[†]Corresponding author: fadhel.alabdullah@alasala.edu.sa

improve the barrier properties of polymer coatings. Chaudhry et al. studied the electrochemical properties of nanocomposites of graphene and polyvinyl butyral. The electrochemical properties were determined in 4 w/v % of NaCl after immersion in 1 and 12 hours of immersion. As exhibited by Nyquist plots, the improved diffusive nature of the nanocomposite coatings was an indication of improved barrier effect provided by graphene [15]. In another research, nanocomposite coatings based on graphene and water-based epoxy resin were fabricated and applied on 2024-T3 aluminum alloys. The electrochemical impedance spectroscopy (EIS) study showed that addition of small amount of reduced graphene to epoxy resin significantly improves the barrier properties of the neat polymer [16].

The worsening effect of graphene has also been reported in the literature due its higher electrical conductivity and higher position in the galvanic series. The former promotes the conductance of electron whereas later acts as cathodic site for the electrochemical reaction. The use of graphene in coatings may produce a short-term barrier enhancement, however in case of disruption of barrier graphene may act as corrosion promoting agent [17]. Chaudhry et al. also discussed the dual nature of graphene by preparing nanocomposite coatings of unmodified graphene with polymer matrix and applied on carbon steel. Using corrosion monitoring techniques, it was shown that graphene exhibited superior barrier properties for short period of immersion whereas longer immersion indicated worse behavior than the pure polymer matrix. They also discussed the role of graphene in developing connectivity of electrical paths for charge transfer which aided the corrosion promotion. Pure polymer usually act as insulator against the transfer of charge from metal through polymer coating but presence of graphene usually provides active paths for charge transfer [11]. All the previous discussion showed that use of graphene for corrosion protection could be risky for long term protection of metals against corrosion [18]. It can be believed that using h-BN will perform same function

without risk of promoting the corrosion reactions due to its insulating properties.

In this research work, we used bath sonicated h-BN as anti-corrosion filler which can improve the barrier properties of polymer coating. The h-BN was bath sonicated for 72 hr to obtain a mixture of particles with large and small lateral dimensions. PVB was dissolved in the solvent contained sonicated h-BN to ensure a proper mixing. Further, corrosion ability of coatings was determined using electrochemical techniques.

2. Materials and Methods

Polyvinyl butyral commercial name Butvar B-98 consisted of 18-20% hydroxyl content was purchased from Sigma Aldrich and used as received. The molecular weight of the as received PVB resin was in range of 40,000-70,000. H-BN (98.0%) micro-powder with average particle size $\sim 5.0 \mu\text{m}$, specific surface area $\sim 7.5 \text{ m}^2/\text{g}$ and true density 2.25 g/cm^3 , was purchased from Graphene Supermarket, USA and used as received. Cold rolled carbon steel, ASTM A1008-15 with composition given in Table 1 was purchased from O'Neal Flat Rolled Metals (OFR Metals), USA and used after surface preparation.

PVB model coatings were prepared by dissolving Polyvinyl butyral, Butvar B-98 (PVB) in Isopropyl Alcohol (IPA) with continuous shaking for 48 hours and then in a sonication bath for few hours. Similarly, different concentrations of h-BN (Table 2), were subjected to sonication in IPA for 72 hr of sonication. PVB was added quickly to the dispersed and exfoliated fillers (Exh-BN) solution and stirred for 48 hours yielded a uniform dispersion of pigment in the PVB solution [19]. Coated carbon steel coupon with dimensions of $25 \times 25 \times 5 \text{ mm}$ and exposed area 2.6 cm^2 and a silver/silver chloride were used as the working electrode and reference electrode respectively. The surface of the carbon steel was prepared by finishing different grades of SiC grit papers from 240 up to 600 grits and polished to a mirror finish. The polished samples were cleaned and degrease with

Table 1. Composition of cold roll carbon steel

C	Mn	P	S	Si	Cu	Ni	Cr	Mo	Al	N	B	Fe
0.036	0.27	0.011	0.01	0.011	0.02	0.01	0.04	0.006	0.051	0.002	0.0002	Bal.

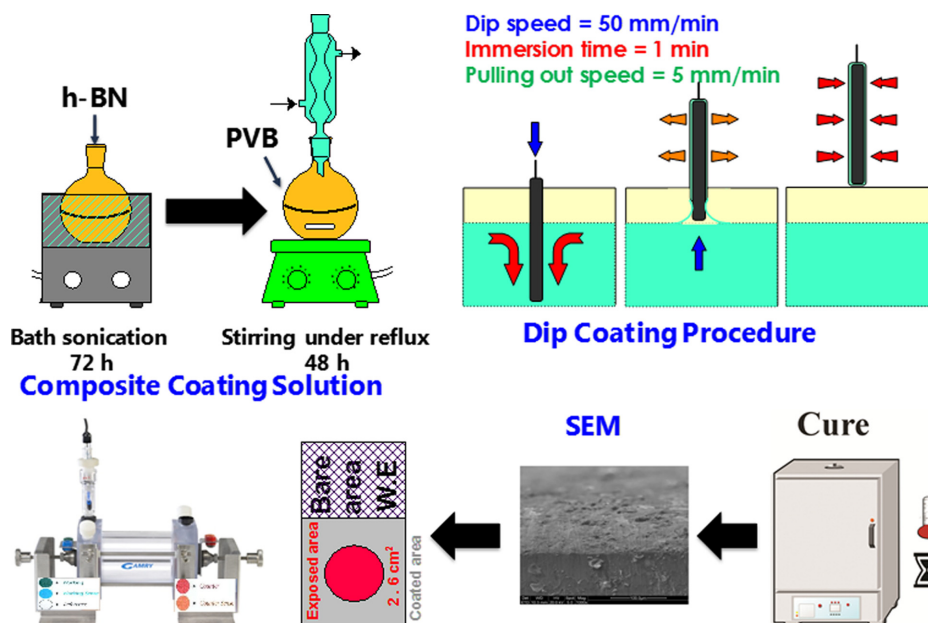


Fig. 1. Coating and electrochemical characterization procedure

Table 2. Composition of the coatings

Filler (h-BN) loading wt%	Code
0.0	P0 (0.0)
0.5	P1 (0.5)
1.0	P2 (1.0)
3.0	P3 (3.0)

industrial grade methanol and acetone, dried in air and stored in incubator for next use. The coated carbon steel substrates were prepared with PVB/filler dispersions using dip coater (Fig. 1) with immersion and withdraw speed of 50 and 5 mm/minute respectively. Further, the samples were dried at room temperature for three days followed by baking in air circulating oven at 175 °C for 2 hours to give final coating with thickness in the range of 80–100 μm. Corrosion studies for coated samples were carried out in 3.5 wt% NaCl solution for different times of exposure.

A three-electrode cell assembly consisting of carbon steel coupon as the working electrode (WE), graphite slab as the counter electrode (CE) and a silver-silver chlorode as reference electrode (RE) were used for the electrochemical measurements. Electrochemical testing such as Open circuit potential (OCP), EIS, and potentiodynamic (PD) was performed in a closed system under naturally aerated

conditions using a Gamry 600 potentiostat/galvanostat/ZRA at room temperature. The sequence of electrochemical techniques is as followed. The OCP of steel samples was recorded against reference electrode. After the completion of each step, EIS and PD were measured by closely following the ref. Impedance measurements were performed as a function of OCP (E_{OCP}) for different time periods. The frequency sweep was done from 10^5 to 10^{-2} Hz at 10 mV AC amplitude [20]. The PD polarization measurements was performed at the end of each experiment by polarizing the working electrode from an initial potential of -250 mV up to a final potential of 750 mV as a function of OCP (E_{OCP}). A scan rate of 0.1667 mV/s was used for the polarization sweep [21,22]. Corrosion current densities were i_{corr} obtained by extrapolating anodic and cathodic linear segments of Tafel plot using Echem Analyst [23].

3. Results and Discussion

3.1 Morphological Characterization

The SEM of h-BN fillers (without sonication) and TEM of bath sonicated h-BN can be seen in Fig. 2. h-BN was bath sonicated in IPA for 72 hr before PVB was incorporated into h-BN suspension. For sonication medium, isopropyl alcohol was used which can also dissolve the polymer resin as well. For exfoliation of h-BN many methods were proposed like chemical, thermal exfoliation, sonication

etc. Among them, sonication is easiest and economical method to achieve Exh-BN 2D sheets [24]. It can be believed that mixture of exfoliated and mostly un-exfoliated can be generated using sonication method. Although we have not presented any quantitative evidence here about the presence of Exh-BN. But in literature sonication is common method to produce Exh-BN h-BN sheets. In our case we used a long sonication time to ensure that resultant suspended material should have a mixture of exfoliated and unexfoliated material. In one of the cited literatures, Khan et al. exfoliated the h-BN using ultrasonic technique in aqueous solutions in the presence of polyvinyl alcohol and produced polyvinyl alcohol/Exh-

BN nanocomposite films. They reported that the resultant Exh-BN nanosheets were sterically stabilized by adsorbed polymer chains on the surface. The characterization showed that the 2D nanosheets were well dispersed in the nanocomposites [25]. The SEM of un-exfoliated bulk h-BN can be seen in . The particle size for 5 μm has some of the lateral dimensions are more than 10 μm indicating a higher surface area. It can be clearly seen that micro sized h-BN having larger lateral size can yield sheets with larger lateral dimension. The high aspect ratio may be useful to improve the barrier properties marginally compared. TEM characterizations of Exh-BN 2D sheets can be observed as semi-transparent indicating a small thickness of stacked sheets. Moreover, the sonication assisted exfoliation process in IPA resulted in few-layers h-BN micro sheets (lateral direction) which were distributed randomly [26]. Lin et al. chemically exfoliated the h-BN into few-layered and monolayered nanosheets using lipophilic and hydrophilic amine molecules. The high resolution TEM results shows that the Exh-BN nano sheets tends to buckle and fold like our case (Fig. 2). The lateral dimensions were found less than 100-1000 nm [27].

The cross-sectional areas of composites coatings comprised of partially Exh-BN with 5.0 μm particle size can be seen in Fig. 3. The cross-sectional areas do not show any major agglomeration at micro level. Otherwise, it can be believed that the nanocomposites coatings contained well dispersed h-BN particles.

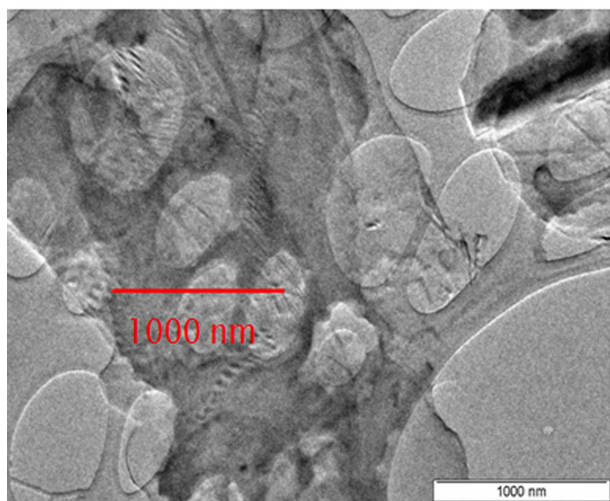
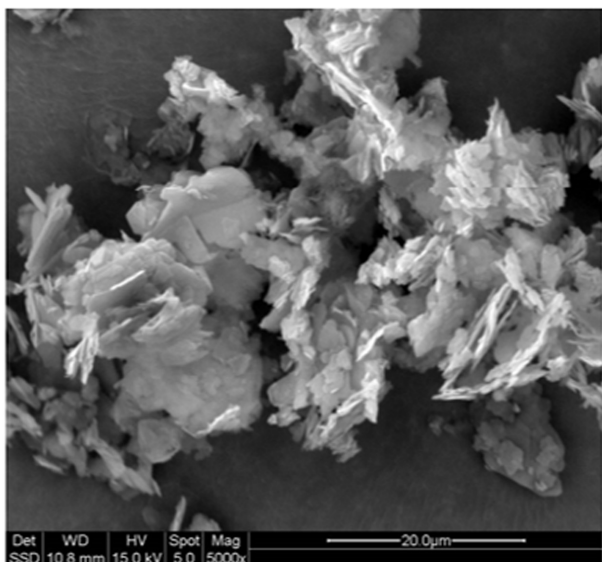


Fig. 2. SEM and TEM for h-BN and 72 hr Sonicated h-BN respectively

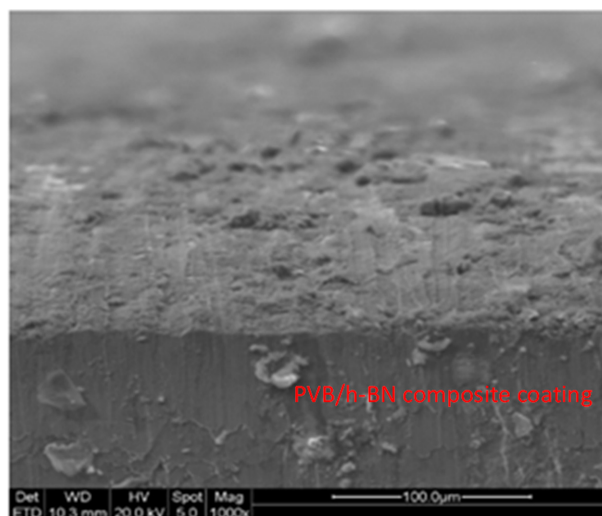


Fig. 3. SEM of cross section of composite coating containing 5.0 μm h-BN

3.2 Electrochemical characterization

The electrochemical properties of the composite coatings were evaluated using electrochemical techniques such as OCP, EIS, and PD. OCP measurements were performed after different periods of immersion such as starting from 1 hour up to 72 hours. After every OCP step, EIS was conducted and finally PD was conducted at the end i.e., after 73 hr of exposure time. Various loading of h-BN i.e. from 0.5 to 3 wt% of PVB were used to study the effect the addition of h-BN on PVB barrier properties.

3.2.1 Open Circuit Potential

Usually, the OCP measurements determine the corrosion potential of the coated metals against a reference electrode with exposing time. In case the OCP values decrease with time, it can be concluded that the coating is degrading and developing electrolyte ionic paths [28]. Table 3 and Fig. 4 present the OCP values of neat PVB and composite coatings evolved during immersion of 72 hr in saline solution. It can be seen that the OCP value of pure PVB coating began at -560 mV after 12 hr and increased to -272 mV after 36 hr, demonstrating that the PVB resin has a healing effect. After that, it continuously decreasing towards negative direction and ended at \sim -340 mV indicating the exhausted healing effect of neat PVB. This kind of healing also shown by one of the researcher where the pure PVB coating showed decline and then returned to positive value and became stable [29]. Arayachukiat et al. reported the enhanced self-healing behavior of PVB even without any chemical reaction in the presence of water. They attributed the enhanced healing effect in the presence of water to the marked molecular motion due to surface localization of vinyl alcohol at surface/defects. During this physical reaction the water acts as a plasticizer [30]. The healing effect of the pure PVB would also be considered in the proceeding discussion of composite coatings as generally addition of fillers improves the

barrier properties of polymer coatings. Also, during the OCP measurements fluctuations were observed in all of the profiles which is common in case of metal covered with coatings and immersed for a long period of time [12].

The addition of 0.5 wt. % of 72 hr bath sonicated h-BN improves the potential of the nanocomposite coatings from \sim -560 mV (PVB) to \sim -453 mV after 12 hr exposed to corrosive solution indicating the slightly improved barrier effect provided by plate-like nature of the sonicated h-BN. Further, the OCP displayed a major change in the OCP value at 24 hr indicating the earlier healing effect compared to blank PVB where it was observed at 36 hr. The OCP trend displayed a negative trend after 36 hr, and ended at -367 mV which is slightly lower than pure PVB coating. It can be said that addition of lower loading of h-BN favoring the healing effect of PVB resin to some extent and shifting the onset of healing effect towards shorter period of immersion. Also, the healing effect was more pronounced than neat PVB coatings. These results may be attributed to the nucleating effect provided by sonicated h-BN to accelerate the surface localization of

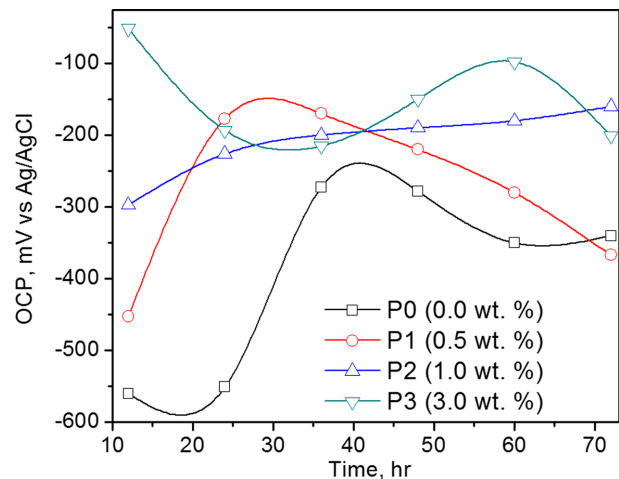


Fig. 4. Evolution of OCP of polymer composite coatings during 72 hr of immersion exposed to 3.5% NaCl

Table 3. OCP for polymer composite coatings during 72 hr of immersion exposed to 3.5% NaCl

	Sample Code & Time (hr)	12	24	36	48	60	72
OCP (mV)	P0 (0.0)	-560	-551	-272	-278	-350	-340
	P1 (0.5)	-453	-177	-170	-220	-280	-367
	P2 (1.0)	-297	-226	-200	-190	-180	-160
	P3 (3.0)	-51	-193	-215	-150	-98	-201

vinyl alcohol as mention during neat PVB coating discussion.

Moreover, increasing the loading of sonicated h-BN to 1.0 wt% exhibited an improved OCP values i.e. from -560 mV (PVB) to -297 mV after 12 hr indicating improved barrier effect of filler whereas during 24 hr to 36 hr coating displayed rise in the OCP towards positive direction and ended at -167 mV indicating the marked healing effect of composite coating as seen in case of individual PVB coating and P1. Increasing the amount of h-BN to 3 wt.%, the barrier properties were largely improved i.e. -560 mV (PVB) to -51 mV after 12 hr of immersion and continue to decrease towards negative direction and ended at -201 mV slightly higher than P2 after 72 hr. It is noteworthy that addition of unfunctionalized filler at higher loading may result in the poor dispersion and interaction of filler to polymer chains sometimes provides easy passages for the corrosive species to enter in the coatings [31]. The lower OCP values and delayed healing effect in case of P3 coating may attributed to the presence of relatively higher number of paths for corrosive species as indicated by huge positive shift in case of P3 at 60 hr of immersion.

From the OCP results the protection mechanism provided by composites coatings can be attributed towards the barrier properties of h-BN. Neat polymer coatings/films have defects as well free volume due to polymer structure. The diffusivity of the corrosive solution through the polymer film especially through the free volume and defects (arise during application). Presence of fillers most importantly high aspect ratio fillers in the polymer coating can reduce the polymer film free volume and defects in the coating. Additionally, polymer is famous for their insulating behavior and does not promote the conduction of electron through the coating to reach other corrosion site. Presence of a conductive filler in the coating may promote the electrochemical processes occurring at the interface for longer period of exposure. Since h-BN is electrically insulating filler, contrary to graphene it will not have affect in promoting the electrochemical reaction occurring on the surface. indicates the corrosion protection mechanism offered by high aspect ratio fillers. The high aspect ratio filler when incorporated in polymers not only reduce the defect in the coatings but also slow down the penetration of the corrosive species through polymer coatings by providing longer diffusion paths. As indicated by composite

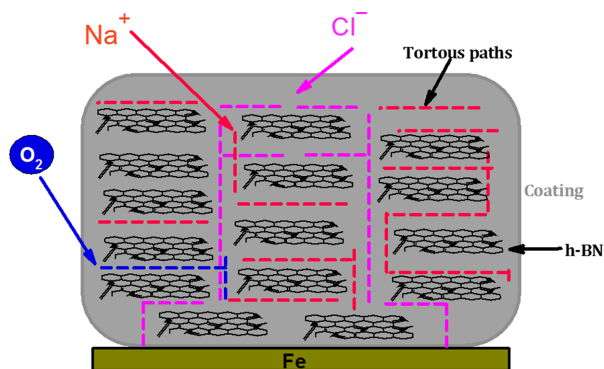


Fig. 5. Protection mechanism offers by composite coatings

coatings containing 1.0 wt% and 3.0 wt% of dispersed h-BN, initial blocking effect of the composites was marginally improved with increased loading of h-BN. Also presence of filler with non-functional surface may result poor interaction of filler surface and polymer chain which can result poor barrier properties of polymer composite coating. As we observed that at higher loading of h-BN i.e. 3.0 wt%, the ended OCP value was lower than 1.0 wt% indicating relatively poor dispersion and lack of filler interaction with the polymer [6].

3.2.2 Electrochemical Impedance Spectroscopy

EIS studies were conducted to understand the electrochemical process in the coating and at the interface. The coating/layer resistance depends on the ability of the polymer to resist the development of ionic pathways with in the coating. The higher the number of ionic paths exist in the coating lower resistance of the coatings. The polymer usually has free volume between polymer chains which provides the easy paths for the electrolyte molecules to penetrate through it. Moreover, there are other factors such as solubility parameter, temperature, corrosive nature of solvent, interaction of polymer chains with solvent molecules etc. also effect the film resistance of the coating towards corrosive solution [15].

The EIS spectra of the polymer and composites coatings were analyzed using circuit models given in Fig. 6. In this equivalent circuit models, generally R_u accounts for the uncompensated electrolyte resistance; R_{pore} and R_{el} describe the coating pore resistance and metal characteristics respectively, Y_c , a_c and Y_{cl} , a_{cl} represent the constant phase element (CPE) constants for coating and double layer capacitance respectively [9,12,32]. The impedance

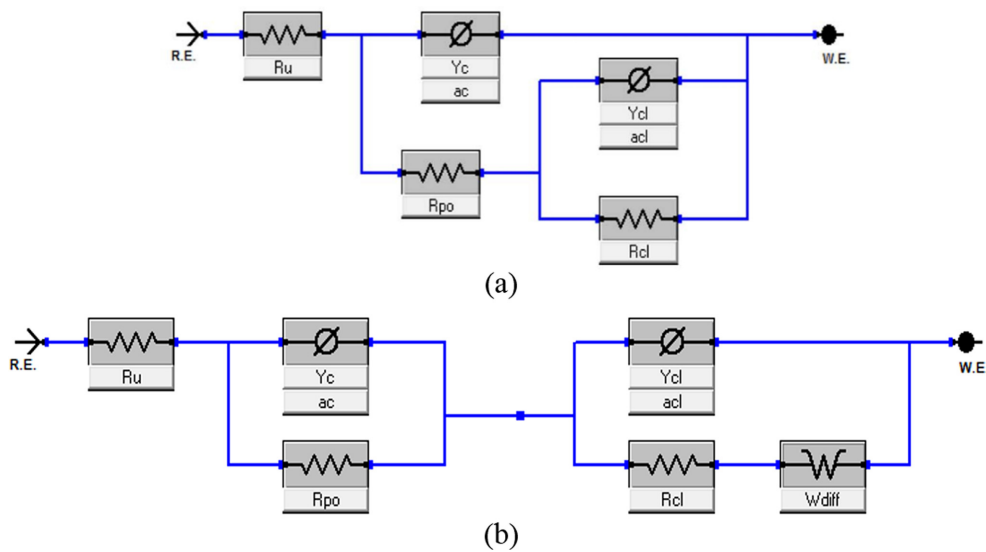


Fig. 6. Model circuits for (a) PVB, 0.5 wt% and 3 wt% h-BN and (b) 1.0 wt% h-BN composites coatings on carbon steel during immersion in 3.5% NaCl

of the CPE can be calculated using following equation $Z(CPE) = Y_0^{-1}(j\omega)^n$. where, Y_0 is the constant of CPE, ω is the angular frequency in rad s^{-1} , and n is the exponential term which can vary between 1 for pure capacitance and 0 for a pure resistor. n is a measure of surface in homogeneity; the lower its value, the higher is the surface roughening of the metal/alloy [11,20,33,34]. From this equation, the capacitance of the coating can be calculated using equation $CPE = Y_0(j\omega)^{1-n}$. Also to simulate the semi-infinite linear diffusion behavior Warburg element was also introduced in one of the two model circuits. The Warburg diffusion element can be calculated as $Z_{diff} = \{1/Y_d \times \sqrt{\omega}\}$ where Y_d is the magnitude of admittance and ω is the angular frequency [32].

Moreover, the protection behavior of the coated metal may be inferred from the combined resistance of the coating and charge transfer resistance of the metallic surface. The coating resistance indicate the resistance of the ionic paths present in the coating during exposure to the corrosive solution. The charge transfer resistance indicates the ability of the metal surface to resist the electrochemical reaction to occur on the surface i.e., at the interface of coating and metal. Usually, the metal resistance is directly affected by the resistance provided by the coating. In case the coating has good resistance, it may stop the corrosive solution to reach the interface; consequently, improves the charge transfer resistance.

Also, the values of impedance (y-axis) at frequency approaching to zero ($f \rightarrow 0$) usually represent the combined resistance provided by coating and metallic surface [35,36].

Fig. 7 present the EIS plots (Bode and Nyquist) and parameters blank PVB coatings exposed to 3.5 wt% NaCl for two periods of immersion i.e., 12 hr and 72 hr These values were obtained after simulating the EIS data using the model circuit shown in Fig. 6. The Bode phase angle of blank PVB coating exhibited a typical plot of metal coated with polymer coating i.e. at higher frequency range dominant capacities behavior, mixed capacitive and resistive behavior at intermediate frequency range and dominant resistive behavior at lower frequency. Similarly, Nyquist plots for PVB exhibited two semicircles corresponding to two reactive components of coating and metallic surface. However, Nyquist plot after 72 hr of immersion at low frequency showed flattening of capacitive loop indicated a hint of diffusion behavior. It can be seen that R_p of pure PVB coating exhibited a resistance of $1.5E7 \Omega\text{cm}^2$ after 12 hr which showed a slight decline to $1.1E7 \Omega\text{cm}^2$ after 72 hr immersion exhibiting the good barrier properties of coating for relatively longer periods immersion. However, resistance of metallic substrate showed a slight improvement after 72 hr of immersion. This may be attributed to two different phenomena, firstly corrosion product forming on the

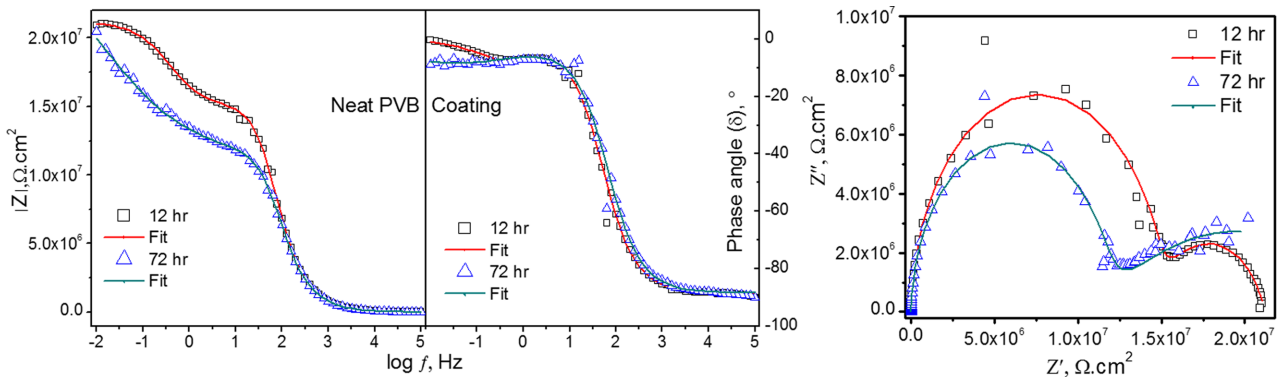


Fig. 7. EIS plots fitted with model circuit (left) Bode and (right) Nyquist for Blank PVB coating obtained after 12 hr and 72 hr of immersion in 3.5 wt% NaCl aqueous solution

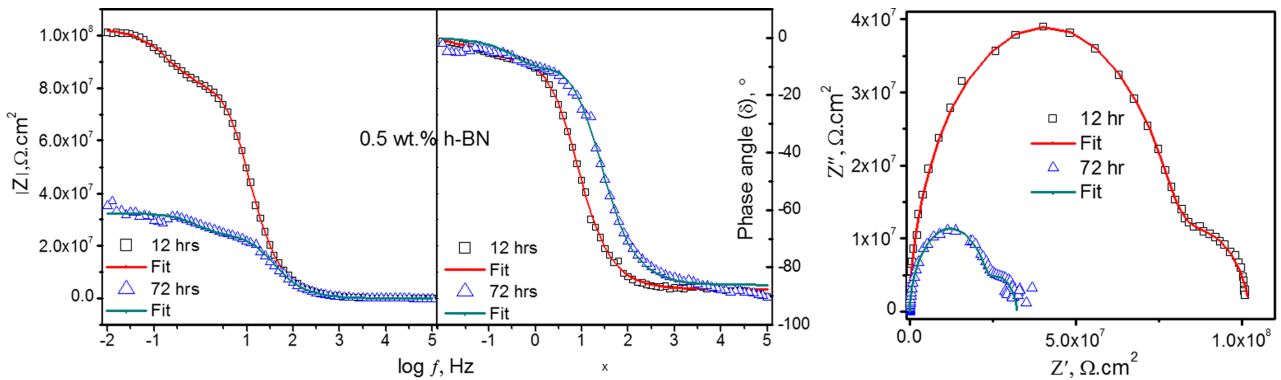


Fig. 8. EIS plots fitted with model circuit (left) Bode and (right) Nyquist for 0.5 wt% h-BN PVB composites coatings obtained after 12 hr and 72 hr of immersion in 3.5 wt% NaCl aqueous solution

metal surface blocking the pores in coating at interface, secondly the self-healing ability of PVB coatings at metal-coating interface. This phenomenon is more pronounced at low frequency range of Nyquist plot where a hint of diffusion can be observed as indicated by long diffusion tail at low frequency range. Also, the phase angle of bode plots indicates slight depression from 0° towards negative angle i.e. -15° at low frequency range indicating dominant capacitive-diffusive behavior. Moreover from Table 4 it can be seen that the slight increase in the coating capacitance after 72 hr also indicates that the presence of corrosive species in the coating whereas the marginally increase double layer capacitance also indicates that presence of corrosive species along with water has reached at the interface. We have already discussed in OCP section that water act as a plasticizer during healing of PVB coating. These results indicate that water reaching at coating-metal interface improving the healing of PVB resulting improved charge transfer resistance.

The addition of 0.5 wt% sonicated h-BN to PVB improved the resistance of coating by almost 5 times and remained higher after 72 hr of immersion compared to blank PVB. On the other hand compared to blank PVB the coating resistance of 0.5 wt% deteriorating rapidly indicating the effect of h-BN on PVB healing abilities. This behavior can be observed in bode phase angle (Fig. 8) where the mixed capacitive-resistive behavior was shifting from lower (12 hr) to higher (72 hr) frequency range and also found a little depression at very low frequency in case 72 hr immersion indicating a presence of small blisters near the metallic surface. These results can also be confirmed by a relatively lower Rcl values after 72 hr However, double layer capacitance showed an improved value compared to 12 hr of immersion.

Further, increasing the loading of sonicated h-BN to 1 wt% improved the coating resistance marginally i.e. $1.5E10 \text{ } \Omega\text{cm}^2$ and exhibited a highest value among all other compositions. This effect can also be seen in Bode

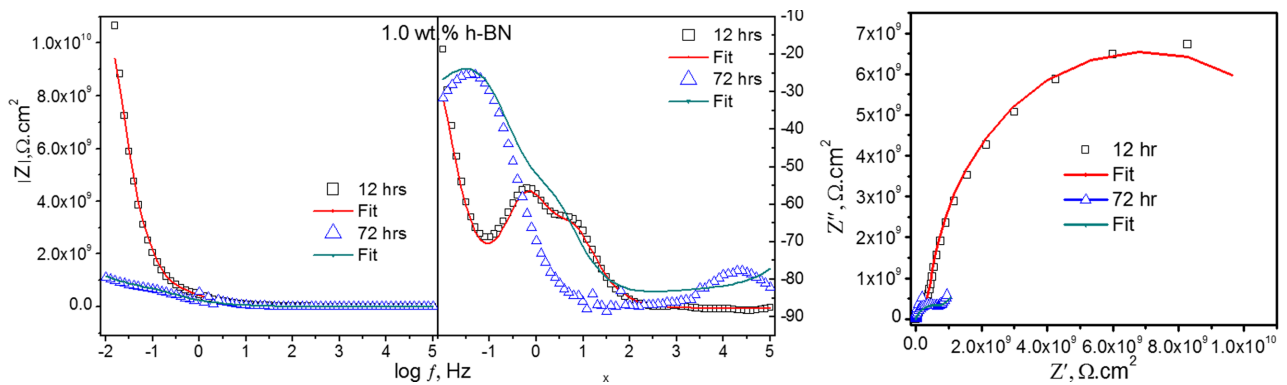


Fig. 9. EIS plots fitted with model circuit (left) Bode and (right) Nyquist for 1.0 wt% h-BN PVB composites coatings obtained after 12 hr and 72 hr of immersion in 3.5 wt% NaCl aqueous solution

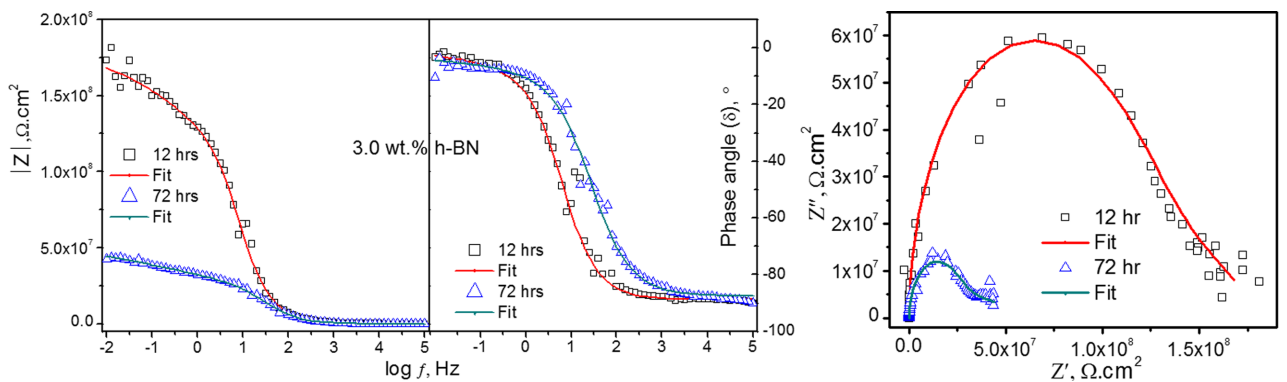


Fig. 10. EIS plots fitted with model circuit (left) Bode and (right) Nyquist for 3.5 wt% h-BN PVB composites coatings obtained after 12 hr and 72 hr of immersion in 3.5 wt% NaCl aqueous solution

Table 4. EIS parameters for polymer nanocomposite coatings for 12 hr and 72 hr of immersion in 3.5% NaCl in 3.5% NaCl aqueous solution

EIS parameters		Rp (Ω.cm²)		Rcl (Ω.cm²)		Cc F/cm²		Cdl F/cm²	
Time (hr)		12	72	12	72	12	72	12	72
SMP.	P0 (0.0)	1.5E7	1.1E7	6.1E6	1.6E7	2.5E-10	2.5E-10	3.5E-7	6.0E-6
	P1 (0.5)	8.0E7	2.3E7	2.1E7	8.8E6	3.2E-10	4.2E-10	1.4E-7	5.0E-8
	P2 (1.0)	1.5E10	5.2E8	1.3E9	1.2E7	3.79E-10	3.14E-09	7.8E-10	4.3E-10
	P3 (3.0)	9.4E7	2.73E7	8.7E7	1.51E7	2.5E-10	4.48E-10	2.8E-7	1.02E-7

phase angle (Fig. 9) where highly capacitive and diffusional behavior was observed at low frequency range. Moreover, a large capacitive loop was also observed in Nyquist plots. On the other hand after 72 hr the coatings resistance exhibited a value of 5.2E8 Ω.cm² which was also highest among all other compositions.

Upon increasing the loading of sonicated h-BN to 3.0 wt% in polymer coatings, we observed degradation of

coating resistance relative to 1.0 wt% of h-BN as indicated by Fig. 10 and impedance values given in Table 4 but still higher than other compositions. As discussed earlier that addition of unfunctionalized h-BN results poor interaction between polymer chains and filler surface. Higher loading of h-BN particles could also result large number of defects in the coating hence deteriorating the coating resistance.

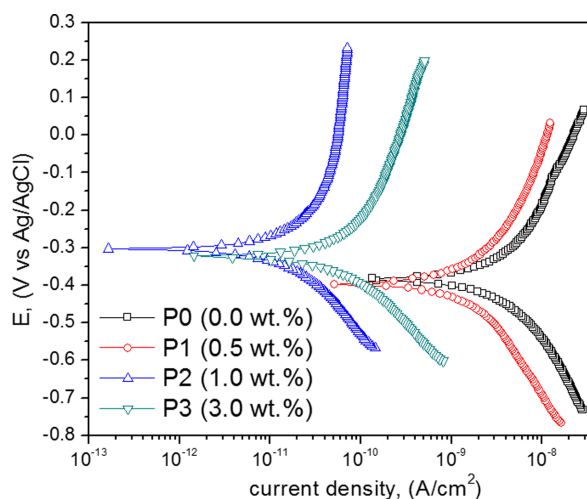
Table 5. Potentiodynamic polarization parameters of polymer nanocomposite coatings after 73 hr of immersion exposed to 3.5% NaCl aqueous solution

Sample	Current density (A/cm ²)	Corrosion Potential (mV)	CR (mm/year) × 10 ⁻⁶
P0 (0.0)	1.6E-9	-380	743
P1 (0.5)	5.1E-10	-390	233
P2 (1.0)	2.6E-12	-303	1.2
P3 (3.0)	1.0E-11	-323	4.8

3.2.3 Potentiodynamic

Corrosion/exchange current density (i_c) is one of the useful information which is extracted from potentiodynamic polarization (PP) curves by extrapolating back from the anodic and cathodic branches from deviating point to the point where the forward and backward reactions are equivalent [37]. Lower the value of i_c higher it is advantageous to effective anti-corrosion coating. Fig. 11 and Table 5 show the PP curves of coated carbon steel and parameters extracted from PP curves such as exchange i_c , corrosion potential (E_c) and corrosion rate (CR) after exposed to 3.5 wt% NaCl for 73 hr. The immersion time of 73 hr was chosen because as we observed from OCP that healing effect of PVB was exhausted after 72 hr of immersion hence true barrier properties of composites coatings can be anticipated.

Blank PVB coatings showed corrosion current density value as 1.6E-9 and corrosion potential -380 mV which was improved for corrosion current and slightly decreased for potential with the addition of 0.5 wt% of h-BN i.e., 5.1E-10 A/cm² and -390 mV. These results indicate the lower amount of h-BN improves the barrier properties of polymer as shown by OCP and EIS [11]. Further, increasing the loading of h-BN in the PVB composites, decreased the current density to three orders of magnitude indicating the inhibiting effect of sonicated h-BN on PVB coatings. Along with the decreased corrosion current, the presence of 1 wt.% h-BN also caused the potential of coated carbon steel to be shifted in positive direction and exhibited a value of -303 mV. Further, the addition 3.0 wt% h-BN exhibited slightly higher current values than P2 indicating the deteriorated barrier properties of composites coatings. It was earlier reported that relatively reduced corrosion current might have resulted from the poor barrier properties due to imperfect interaction of the unfunctionalized fillers to the PVB matrix, which caused the formation of additional diffusional pathways at filler-polymer interfaces [31].

**Fig. 11. Potentiodynamic polarization curves of samples coated with PVB and nanocomposites coatings recorded after 73 hr of immersion in 3.5% NaCl aqueous solution**

4. Conclusions

This research work deals with the investigation of electrochemical properties of sonicated h-BN based composite coatings containing different loading of mixture of exfoliated and un-exfoliated h-BN applied on carbon steel. To study the effect of barrier properties, we selected 5 μm particle size of h-BN and sonicate it for 72 hr in isopropyl alcohol. The composites coatings were generated by dissolving the polyvinyl butyral resin in the solution containing mixture of sonicated h-BN. The corrosion properties were studied in 3.5 wt% NaCl viz different electrochemical studies such as open circuit potential, electrochemical impedance spectroscopy and potentiodynamic. The TEM confirmed presence of Exh-BN. The TEM images showed that Exh-BN obtained from 5 μm particles exhibited lateral dimension in micrometric size. The h-BN to nanocomposite coatings marginally improved the corrosion properties for shorter and longer period of immersion. These results indicate that exfoliated

HBN with larger lateral dimension could be used as replacement of graphene in polymeric coatings for anti-corrosion purposes.

References

1. A. U. Chaudhry, R. Bhola, V. Mittal, and B. Mishra, Ni_{0.5}Zn_{0.5}Fe₂O₄ as a Potential Corrosion Inhibitor for API 5L X80 Steel in Acidic Environment, *International Journal of Electrochemical Science*, **9**, 4478 (2014). Doi: <http://www.electrochemsci.org/papers/vol9/90804478.pdf>
2. X. Wang, C. Xu, Y. Chen, C. Tu, Z. Wang, and X. Song, Effects of stray AC on corrosion of 3-layer polyethylene coated X70 pipeline steel and cathodic delamination of coating with defects in 3.5 wt% NaCl solution, *Corrosion Engineering, Science and Technology*, **53**, 214 (2018). Doi: <https://doi.org/10.1080/1478422X.2018.1436736>
3. H. Rahman, and S. J. Zaidi, Desalination in Qatar: Present Status and Future Prospects, *Civil Engineering Research Journal*, **6**, 555700 (2018). Doi: <http://doi.org/10.19080/CERJ.2018.06.555700>
4. AU Chaudhry, Abdel Nasser Mabrouk and Ahmed Abdala, Thermally enhanced polyolefin composites: fundamentals, progress, challenges, and prospects, **21**, 737 (2020). <https://doi.org/10.1080/14686996.2020.1820306>
5. M. Rajabi, G. R. Rashed, and D. Zaarei, Assessment of graphene oxide/epoxy nanocomposite as corrosion resistance coating on carbon steel, *Corrosion Engineering, Science and Technology*, **50**, 509 (2015). Doi: <https://doi.org/10.1179/1743278214Y.0000000232>
6. W. Wu, J. Liu, X. Li, T. Hua, X. Cong, Z. Chen, F. Ying, W. Shen, B. Lu, K. Dou, and X. Zhou, Incorporation graphene into sprayed epoxy-polyamide coating on carbon steel: corrosion resistance properties, *Corrosion Engineering, Science and Technology*, **53**, 625 (2018). Doi: <https://doi.org/10.1080/1478422X.2018.1521590>
7. V. Mittal, and A. U. Chaudhry, Effect of amphiphilic compatibilizers on the filler dispersion and properties of polyethylene—thermally reduced graphene nanocomposites, *Journal of Applied Polymer Science*, **132**(35) (2015). Doi: <https://doi.org/10.1002/app.42484>
8. V. Mittal, A. U. Chaudhry, and M. I. Khan, Comparison of Anti-Corrosion Performance of Polyaniline Modified Ferrites, *Journal of Dispersion Science and Technology*, **33**, 1452 (2012). Doi: <https://doi.org/10.1080/01932691.2011.620827>
9. A. U. Chaudhry, V. Mittal, and B. Mishra, Impedance response of nanocomposite coatings comprising of polyvinyl butyral and Haydale's plasma processed graphene, *Progress in Organic Coatings*, **110**, 97 (2017). Doi: <https://doi.org/10.1016/j.porgcoat.2017.04.032>
10. A. U. Chaudhry, V. Mittal, and B. Mishra, Nano nickel ferrite (NiFe₂O₄) as anti-corrosion pigment for API 5L X-80 steel: An electrochemical study in acidic and saline media, *Dyes and Pigments*, **118**, 18 (2015). Doi: <https://doi.org/10.1016/j.dyepig.2015.02.023>
11. A. Chaudhry, V. Mittal, and B. Mishra, Inhibition and promotion of electrochemical reactions by graphene in organic coatings, *RSC Advances*, **98**, 80365 (2015). Doi: <https://doi.org/10.1039/C5RA12988E>
12. A. Chaudhry, V. Mittal, M. Hashmi, and B. Mishra, Evaluation of NiO. 5ZnO. 5Fe₂O₄ nanoparticles as anti-corrosion pigment in organic coatings for carbon steel, *Anti-Corrosion Methods and Materials*, **64**, 644 (2017). Doi: <https://doi.org/10.1108/ACMM-10-2016-1725>
13. A. Chaudhry, V. Mittal, and M. Hashmi, A quick review for rheological properties of polyolefin composites, *Sindh University Research Journal-SURJ (Science Series)*, **44**, 75 (2012). <https://sujo-old.usindh.edu.pk/index.php/SURJ/article/view/1399>
14. K. E. Spirydowicz, E. Simpson, R. A. Blanchette, A. P. Schniewind, M. K. Toutloff, and A. Murray, Alvar and Butvar: The Use of Polyvinyl Acetal Resins for the Treatment of the Wooden Artifacts from Gordion, Turkey, *Journal of the American Institute for Conservation*, **40**, 43 (2001). Doi: <https://doi.org/10.1179/019713601806113139>
15. A. Chaudhry, V. Mittal, and B. Mishra, Impedance response of nanocomposite coatings comprising of polyvinyl butyral and Haydale's plasma processed graphene, *Progress in Organic Coatings*, **110**, 97 (2017). Doi: <https://doi.org/10.1016/j.porgcoat.2017.04.032>
16. T. Monetta, A. Acquesta, and F. Bellucci, Graphene/epoxy coating as multifunctional material for aircraft structures, *Aerospace*, **2**, 423 (2015). Doi: <https://doi.org/10.3390/aerospace2030423>
17. F. Zhou, Z. Li, G. J. Shenoy, L. Li, and H. Liu, Enhanced Room-Temperature Corrosion of Copper in the Presence of Graphene, *ACS Nano*, **7**, 6939 (2013). Doi: <https://doi.org/10.1021/nn402150t>
18. L. H. Li, T. Xing, Y. Chen, and R. Jones, Boron nitride nanosheets for metal protection, *Advanced materials interfaces*, **1**, 1300132 (2014). Doi: <https://doi.org/10.1002/admi.201470047>
19. S. Radhakrishnan, C. R. Siju, D. Mahanta, S. Patil, and G.

- Madras, Conducting polyaniline–nano-TiO₂ composites for smart corrosion resistant coatings, *Electrochimica Acta*, **54**, 1249 (2009). Doi: <https://doi.org/10.1016/j.electacta.2008.08.069>
20. C. A. Usman, Anti-corrosion behaviour of barrier, electrochemical and self-healing fillers in polymer coatings for carbon steel in a saline environment, *Colorado School of Mines* (2016). <http://hdl.handle.net/11124/170102>
 21. ASTM-G61-86, Standard Test Method for Conducting Cyclic Potentiodynamic Polarization Measurements for Localized Corrosion Susceptibility of Iron-, Nickel-, or Cobalt-Based Alloys, ASTM International: West Conshohocken, PA (2009).
 22. ASTM-G3-89, Standard Practice for Conventions Applicable to Electrochemical Measurements in Corrosion Testing, ASTM International (2010).
 23. D. Asefi, M. Arami, and N. M. Mahmoodi, Effect of Chain Length Compatibility between Surfactants and Co-Surfactants on Corrosion Inhibition of Steel, *ECS Transactions*, **35**, 1 (2011). Doi: <https://doi.org/10.1149/1.3647848>
 24. L. Song, L. Ci, H. Lu, P. B. Sorokin, C. Jin, J. Ni, A. G. Kvashnin, D. G. Kvashnin, J. Lou, and B. I. Yakobson, Large scale growth and characterization of atomic hexagonal boron nitride layers, *Nano letters*, **10**, 3209 (2010). Doi: <https://doi.org/10.1021/nl1022139>
 25. U. Khan, P. May, A. O'Neill, A. P. Bell, E. Boussac, A. Martin, J. Semple, and J. N. Coleman, Polymer reinforcement using liquid-exfoliated boron nitride nanosheets, *Nanoscale*, **5**, 581 (2013). Doi: <https://doi.org/10.1039/C2NR33049K>
 26. Z. Lin, A. Mcnamara, Y. Liu, K.-S. Moon, and C.-P. Wong, Exfoliated hexagonal boron nitride-based polymer nanocomposite with enhanced thermal conductivity for electronic encapsulation, *Composites Science and Technology*, **90**, 123 (2014). <https://doi.org/10.1016/j.compscitech.2013.10.018>
 27. Y. Lin, T. V. Williams, and J. W. Connell, Soluble, exfoliated hexagonal boron nitride nanosheets, *The Journal of Physical Chemistry Letters*, **1**, 277 (2009). Doi: <https://doi.org/10.1021/jz9002108>
 28. L. Jinlong, L. Tongxiang, W. Chen, and D. Limin, Surface corrosion enhancement of passive films on NiTi shape memory alloy in different solutions, *Materials Science and Engineering: C*, **63**, 192 (2016). Doi: <https://doi.org/10.1016/j.msec.2016.02.066>
 29. B. Mishra, A. Chaudhry, and V. Mittal, Development of Polymer-Based Composite Coatings for the Gas Exploration Industry: Polyoxometalate Doped Conducting Polymer Based Self-Healing Pigment for Polymer Coatings, *Materials Science Forum*, **879**, 60 (2016). <https://doi.org/10.4028/www.scientific.net/MSF.879.60>
 30. S. Arayachukiat, V. A. Doan, T. Murakami, S. Nobukawa, and M. Yamaguchi, Autonomic self-healing of poly(vinyl butyral), *Journal of Applied Polymer Science*, **132**, 42008 (2015). Doi: <https://doi.org/10.1002/app.42008>
 31. G. E. Luckachan, and V. Mittal, Anti-corrosion behavior of layer by layer coatings of cross-linked chitosan and poly(vinyl butyral) on carbon steel, *Cellulose*, **22**, 3275 (2015). Doi: <https://doi.org/10.1007/s10570-015-0711-2>
 32. A. U. Chaudhry, B. Mansoor, T. Mungole, G. Ayoub, and D. P. Field, Corrosion mechanism in PVD deposited nano-scale titanium nitride thin film with intercalated titanium for protecting the surface of silicon, *Electrochimica Acta*, **264**, 69 (2018). Doi: <https://doi.org/10.1016/j.electacta.2018.01.042>
 33. A. U. Chaudhry, B. Mishra, and V. Mittal, Graphene for Corrosion Protection, in *Functional Nanomaterials and Nanotechnologies Applications for Energy and Environment*, pp. 207 - 236, V. Mittal, Editor, Central West Publishing: Australia (2018).
 34. S. Chongdar, G. Gunasekaran, and P. Kumar, Corrosion inhibition of mild steel by aerobic biofilm, *Electrochimica Acta*, **50**, 4655 (2005). Doi: <https://doi.org/10.1016/j.electacta.2005.02.017>
 35. Gamry, *Basics of Electrochemical Impedance Spectroscopy*. <https://www.gamry.com/application-notes/EIS/basics-of-electrochemical-impedance-spectroscopy/>
 36. F. T. Alabdullah, Exfoliated hexagonal boron nitride based anti-corrosion polymer nano-composite coatings for carbon steel in a saline environment, *Colorado School of Mines, Arthur Lakes Library* (2018). <https://hdl.handle.net/11124/172804>
 37. D. G. Enos, and L. L. Scribner, The potentiodynamic polarization scan, Technical Report 33, Solartron Instruments, Hampshire, UK (1997). <https://www.ameteksi.com/documentations/technical-report-33>